Geophys. J. Int. (2002) **150,** 724–736

The 1933 $M_s = 7.3$ Baffin Bay earthquake: strike-slip faulting along the northeastern Canadian passive margin

Allison L. Bent

National Earthquake Hazards Program, Geological Survey of Canada, 1 Observatory Cres., Ottawa, Ontario, Canada, K1A 0Y3.
E-mail: bent@seismo.nrcan.gc.ca

Accepted 2002 March 18. Received 2002 March 14; in original form 2001 May 18

SUMMARY

The 1933 November 20 ($M_s = 7.3$) Baffin Bay earthquake is one of the largest instrumentally recorded passive margin earthquakes. Analysis of seismograms of this earthquake shows strong evidence for strike-slip faulting, which contrasts with the generally accepted belief that Baffin Bay is dominated by thrust faulting. The best-fitting solution consists of a large strike-slip subevent (strike 172°, dip 82°, rake 6°) followed by two smaller oblique-thrust subevents (strike 190°, dip 30°, rake 62°). All subevents occur at a depth of about 10 km. An instrumental moment magnitude of 7.4 was determined. Preliminary analysis of subsequent large (magnitude $\geq$6.0) earthquakes in Baffin Bay finds additional evidence for strike-slip faulting in the region. The results for Baffin Bay, together with those for other passive margin earthquakes, suggest strike-slip faulting may be more prevalent in these regions than was previously believed.

Key words: earthquake source mechanism, passive margin, waveform analysis.

INTRODUCTION

The earthquake ($M_s = 7.3$) that occurred beneath Baffin Bay on 1933 November 20 (23:21:35.7 UT, 73.07°N, 70.01°W; Fig. 1) is the largest instrumentally recorded earthquake to have occurred along the passive margin of North America and, possibly the largest passive margin earthquake worldwide. Coincidentally, it is also the largest known earthquake north of the Arctic Circle. Despite its importance, this earthquake has not been as well studied as most other large eastern Canadian earthquakes.

In spite of its size, the 1933 earthquake did not result in any damage because of its offshore location combined with the sparse population of the adjacent onshore areas. There are no known felt reports from Baffin Island or elsewhere in northern Canada. On the other hand, there are no reports to confirm that the earthquake was not felt. Belatedly, the *London Times* (1933 November 28) reported briefly that the earthquake had been felt in Greenland (Fig. 1) in the region from Upernivik to southern Upernivik (a distance of roughly 65 km), but not in either Thule (560 km north of Upernivik) or Disko Bay (480 km south of Upernivik). Very few details were provided, but the absence of any mention of even superficial damage suggests that the intensity in the Upernivik region (550 km from the epicentre) was no more than IV on the modified Mercalli scale.

Prior to this earthquake Baffin Bay had been believed to be aseismic, but subsequent improved seismic monitoring in northern Canada has shown the Baffin Bay region to be very active (Basham *et al.* 1982; also see Fig. 1 of the present paper). Subsequent to 1933, there have been four earthquakes of magnitude 6.0 or greater in Baffin Bay and one on Baffin Island. Qamar (1974) suggests that the Baffin Bay events are aftershocks of the 1933 earthquake and not independent events. Current Canadian seismic hazard maps (Basham *et al.* 1997) show the hazard in Baffin Bay to be comparable to that of coastal British Columbia although, obviously, the risk to the population is considerably lower.

Based on a small number of existing focal mechanisms, it has generally been believed that Baffin Bay is dominated by thrust faulting while earthquakes on Baffin Island are normal faulting events (Stein *et al.* 1979, 1989). The results of the present study based on detailed waveform modelling of the 1933 earthquake and analysis of first-motion data from subsequent large earthquakes, however, provide strong evidence for strike-slip faulting in Baffin Bay.

REGIONAL SEISMOTECTONICS

It had been believed that Baffin Bay was formed by seafloor spreading between 60 and 40 Ma (Jackson *et al.* 1979), but more recent evidence suggests that the seafloor spreading began much earlier-around 69 Ma (Roest & Srivastava 1989). Wetmiller (1974) used the absence of *Lg* waves from earthquakes for which wave trains crossed the centre of the bay to infer that it is still underlain by oceanic crust. It has been difficult to precisely define the ocean–continent boundary owing to the thick sediments in Baffin Bay (Keen *et al.* 1972a). There is evidence for faulting in the basement rocks and older sediments in Baffin Bay (Keen *et al.* 1972a) and for slumping, which could be seismically related, in the younger sediments (Keen *et al.* 1972b).

Although Baffin Bay is now known to be a very active seismic zone, considerably less is known about it relative to the seismic zones in southern Canada. Prior to the 1933 earthquake, the region

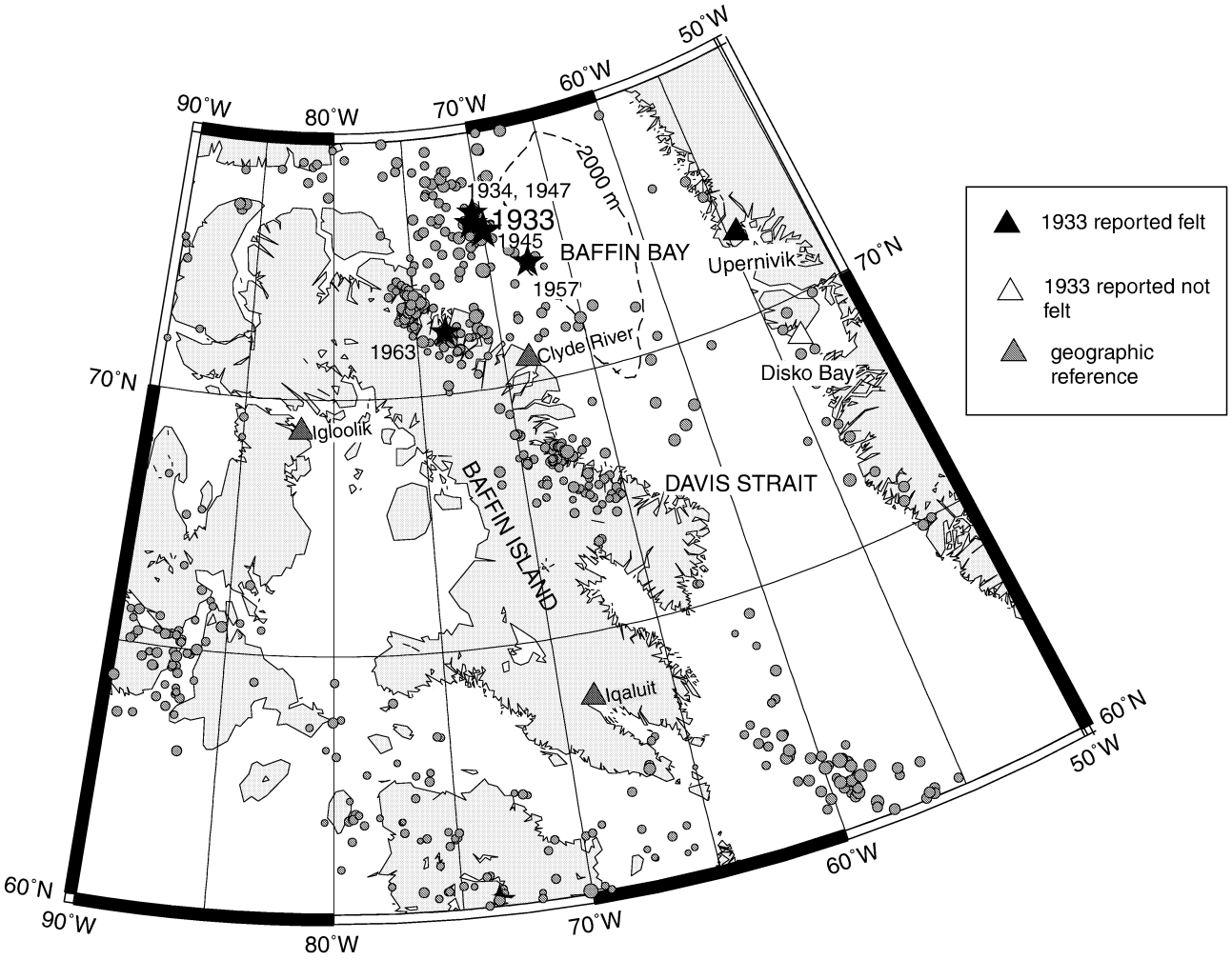

Figure 1. Seismicity in and near Baffin Bay. Circles (scaled to magnitude) indicate epicentres of earthquakes of magnitude less than 6.0. Larger earthquakes are represented by stars and date. Earthquakes of magnitude 5.0 and greater are plotted for the period 1900–1996, magnitudes 4.0–4.9 for 1960–1996, 3.0–3.9 for 1970–1996 and 2.0–2.9 for 1980–1996. See the text for completeness periods for various magnitudes. Epicentres are from the Canadian Earthquake Epicentre File (CEEF). The 2000 m bathymetry contour is indicated by the dashed line. Black triangles indicate communities in which the *London Times* reported that the 1933 earthquake had been felt; white triangles are communities in which the earthquake had been reported *not* felt; grey triangles are communities shown for geographic reference only.

was believed to be aseismic (Lee 1937). Earthquakes of magnitude 6.0 and greater subsequent to 1933 (1934, 1945, 1947 and 1957) are noted in the International Seismological Summary (ISS) and similar summaries, but it was only with the expansion of the Canadian seismograph network in the north during the 1950s and 1960s that these earthquakes could be put into any kind of regional context. Basham *et al.* (1982) estimate that the earthquake catalogue for Baffin Bay is complete above the magnitude 7.0 level since 1920, magnitude 5.5 since 1950, magnitude 4.0 since 1968 and is incomplete for magnitudes less than 4.0 for all time periods. This contrasts sharply with the Charlevoix (Quebec) seismic zone in the long-settled St Lawrence Valley where the completeness years for the same magnitude levels are estimated to be 1660, 1900 and 1937, respectively, and where earthquakes of magnitude less than 0.0 can now be routinely located by a dense local seismograph network.

Historical seismic activity is not uniformly distributed throughout Baffin Bay but is concentrated in northwestern Baffin Bay on the Baffin Island side of the 2000 m bathymetric contour (Basham *et al.* 1977; see Fig. 1 of the present paper). To date no one has been able correlate the seismicity with particular geological structures or geophysical anomalies. It has been suggested (for example, Stein *et al.* 1979) that seismicity in the region is related to the stresses associated with post-glacial rebound.

RELOCATION OF EPICENTRES

Although the 1933 earthquake was virtually ignored in Canada at the time of its occurrence, it received more attention elsewhere. The Canadian seismograph station bulletin reports only a few phase readings for stations in eastern Canada with a brief note that they probably corresponded to an earthquake located by the US Coast and Geodetic Survey. Routine locations (Fig. 2) were reported by the International Seismological Summary (ISS), Bureau Central

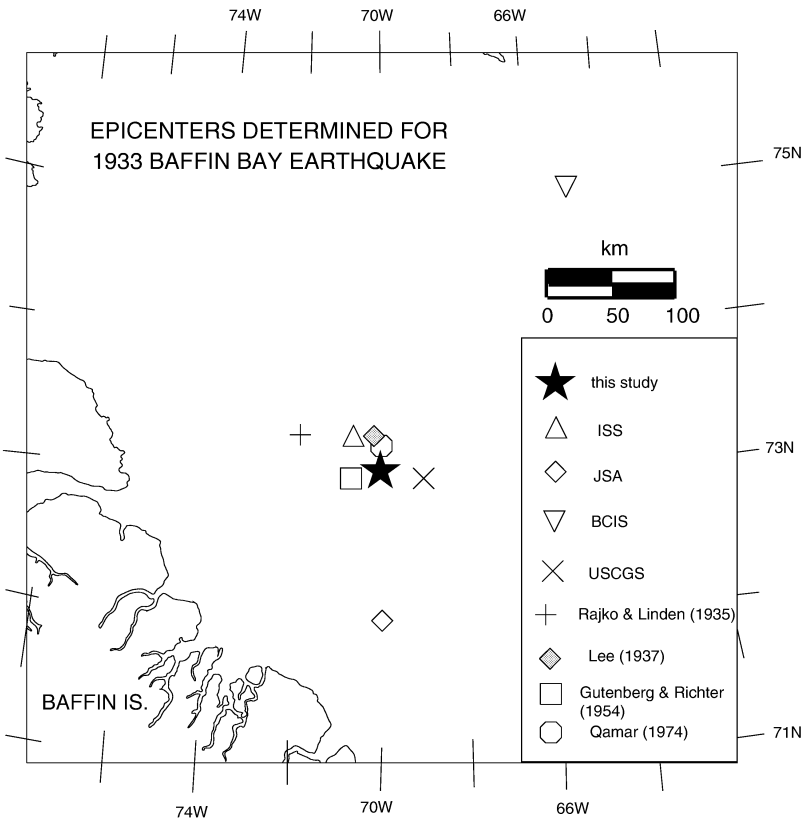

Figure 2. Epicentres of the 1933 Baffin Bay earthquake determined by various sources. ISS is the International Seismological Summary, JSA is the Jesuit Seismological Association, BCIS is the Bureau Central International de Séismologie and USCGS is the US Coast and Geodetic Survey. The uncertainty in the location obtained in this study is of the order of the symbol size.

International de Séismologie (BCIS), the United States Coast and Geodetic Survey (USCGS), the Jesuit Seismological Association (JSA) and by Gutenberg & Richter (1954). The earthquake was relocated as part of several research projects. Rajko & Linden (1935) located the earthquake in a study of Arctic seismicity. Lee (1937), noting that the seismograph stations in North America, Europe and Japan covered a broad azimuthal but narrow distance range, relocated the earthquake in an effort to improve the available traveltime tables, particularly for *S* waves. More recently, Qamar (1974) relocated the 1933 and many other earthquakes in the Baffin Bay–Baffin Island region using the joint hypocentre determination (JHD) method with the 1963 Baffin Island earthquake (200 km from the 1933 event) as the calibration event. Most of the various epicentres for the 1933 earthquake fall in a region roughly 20 km (north–south) by 100 km (east–west) although there are two outliers (Fig. 2).

In this study the epicentres and origin times for the 1933 earthquake and the four subsequent large earthquakes in Baffin Bay were recalculated using an iterative least-squares program (Weichert & Newton 1970), teleseismic *P* arrival times as reported in the ISS and assuming the Preliminary Reference Earth Model or PREM (Dziewonski & Anderson 1981) traveltimes. The ISS appears to have fixed the epicentres of the 1934 and 1947 earthquakes at the epicentres of the 1933 and 1945 events, respectively. Stations with traveltime residuals of more than 60 s were rejected initially, and with each iteration those with residuals greater than 10, 6 and 4 s were subsequently eliminated. The inversion was first performed for each earthquake with no station corrections. Station corrections were then calculated based on the mean residual for each station (or region) from the preliminary relocations, and then the inversion was rerun using the station corrections. Individual station corrections were determined for those stations that reported *P* arrival times for at least four of the five events. Regional corrections were determined for the remaining stations. These corrections, as well as all traveltime residuals, are tabulated in Bent (1998a) and are of the order of a few seconds. In general, corrections were negative at stations in eastern North America and Asia and positive for stations in western North America and Europe. The inclusion of station corrections had only a small effect on the final epicentres. In the most extreme case (the 1947 earthquake) the epicentre moved by about 5 km relative to the first relocated epicentre when the station corrections were added. All events showed slight increases in the number of observations retained and slight decreases in the epicentral and origin time uncertainties when the station corrections were included. The epicentres moved from 8 to 51 km relative to the original ISS epicentres.

A focal depth of 10 km was assumed for all events. The depth of the 1933 earthquake has been determined to be 10 km (see the next section) and the others were assumed to have comparable source depths. Tests to determine the effect of depth on the solution found that depth had a negligible effect on the outcome for upper to mid-crustal hypocentres (Table 1).

The final epicentres as well as the initial ISS locations are shown in Fig. 3, and the epicentral parameters are summarized in Table 2.

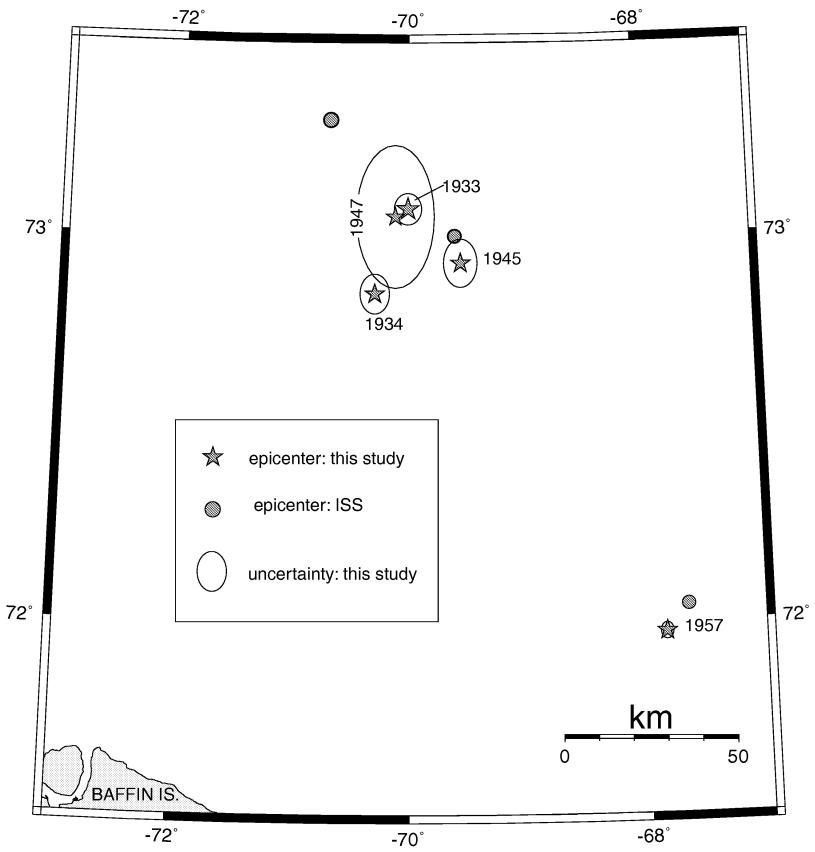

Figure 3. Revised epicentres for Baffin Bay earthquakes of magnitude 6.0 or greater. The original ISS epicentres are also shown.

Table 1. Relocation, effect of depth on epicentre and origin time, examples.

Depth	Lat. (°N)	± (km)	Lon. (° W)	± (km)	OT	± (s)
1933 earthquake						
5	73.05	4.8	69.99	4.1	2321:34.6	0.2
10	73.04	4.8	69.98	4.1	2321:35.4	0.2
15	73.04	4.8	69.98	4.1	2321:36.2	0.2
1947 earthquake						
5	72.93	26	70.08	15	1048:51.1	1.4
10	73.01	26	70.16	14	1048:51.7	1.1
15	73.00	26	70.16	13	1048:52.4	1.1

The revised epicentre for the 1933 earthquake lies near the centre of the cluster formed by previous locations for the event. Traveltime residuals for the 1933 earthquake are shown in Fig. 4; residuals for the other events can be seen in Fig. 5.

SOURCE PARAMETERS

Of the more than 100 stations that reported arrival times to the ISS for the 1933 earthquake, only two (Ivigtut, Greenland and Reykjavik, Iceland) were at distances of less than 20°. Thus the source parameters were determined from teleseismic data.

Analogue seismograms from 15 stations were obtained. The records and instrument parameters are summarized in Table 3 and in more detail by Bent (1998b). The data were hand digitized, corrected for curvature (if necessary) and the horizontal records were rotated into their radial and tangential components.

First motions

The grid search algorithm of Snoke *et al.* (1984) was used to search for the focal mechanism. The *P*-wave first motions read by the author (14 stations) were combined with those reported in the ISS (31 total). One predominantly strike-slip mechanism (Fig. 6) was obtained by searching the focal sphere at 5° intervals. This mechanism contrasts sharply with the mainly thrust mechanisms proposed by Stein *et al.* (1979, 1989) and Kroeger (1991). Searching the focal sphere at smaller intervals did not result in any solutions that differed from the original strike-slip one by more than 3° in any of the three faulting parameters. The strike-slip solution is compatible with the *S* polarities (four *SV* and four *SH*) that could be read. The solution is constrained primarily by dilatational first motions at La Paz (LPB) and Victoria (VIC). Ivigtut (IVI) is also dilatational, but because of the large take-off angle to this station its polarity is compatible with either a strike-slip or thrust mechanism. The LPB first motion was obtained from the ISS and was not verified by this author. If this first motion is excluded from the inversion, a wider range of solutions ranging from pure strike-slip to equal parts thrust and strike-slip are allowed. The first motion at VIC, however, precludes the higher thrust component of Stein *et al.* (1979, 1989) and Kroeger (1991). Pasadena (PAS), which lies near VIC on the focal sphere, has a compressional first motion. The difference in the first motions between VIC and PAS cannot be easily dismissed. The polarities were marked on the seismograms from both stations by the station operators at the time of the earthquake. Both are multicomponent stations and the separate components at each station are mutually consistent (i.e. if the marked polarities are incorrect, they must be

Table 2. Revised epicentral parameters of large earthquakes in Baffin Bay.

Date	Origin time (UT)	± (s)	M_S*	Latitude (deg N)	± (km)	Longitude (deg W)	± (km)	Stations
19331120	23:21:35.7	0.2	7.3	73.07	4.5	70.01	3.7	150
19340831	05:02:49.3	0.2	6.5	72.85	5.5	70.30	4.1	104
19450101	01:20:49.3	0.3	6.5	72.93	6.8	69.55	4.7	62
19470710	10:48:51.3	0.8	6.0	73.05	20.2	70.12	10.8	30
19570502	03:55:37.3	0.1	6.4	71.97	2.3	67.84	1.8	145

Note.—*1957 from Qamar (1974); all others from Gutenberg & Richter (1954).

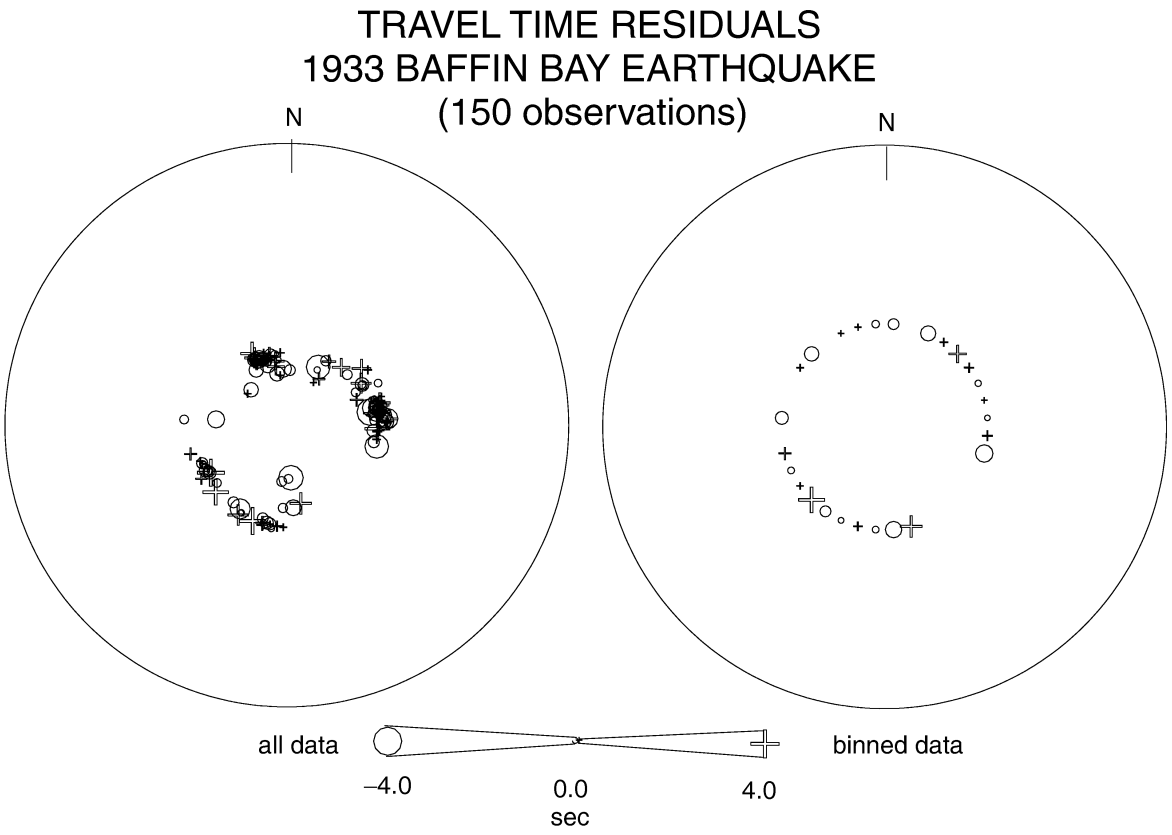

Figure 4. Traveltime residuals after relocation of the 1933 Baffin Bay earthquake. The symbol size is proportional to the residual. Points are plotted on the focal sphere (lower-hemisphere projection). In the figure on the right, data have been binned into 10° azimuthal windows, and the mean residual plotted.

incorrect for all components). Additionally, records from both stations for earthquakes occurring within 5 years in either direction of 1933 have been used in the past by this author and showed no obvious polarity problems. None of these factors completely precludes the possibility of a polarity error, but they suggest that the polarities are reliable.

Waveform modelling

The body waves (both *P* and *S*) were analysed in greater detail using a forward modelling, synthetic seismogram method based on ray summation in the time domain, described in detail by Langston & Helmberger (1975). The synthetic seismogram is defined as the convolution of the instrument response, attenuation, Green's function for wave propagation and the source, where the source is a function of the focal mechanism, scalar moment, depth and far-field time history. A point source of finite duration is assumed but more complex sources can be simulated by adding together two or more point sources. For attenuation, a Futterman (1962) operator, t^*, of 1 s was used to model the *P* waves and 4 s to model the *S* waves. The velocity model used was that of Srivastava *et al.* (1981), which was based on seismic refraction surveys in Baffin Bay.

Neither the first-motion strike-slip mechanism nor the previously proposed thrust mechanisms provided a completely satisfactory fit to the waveforms. Nor did an intermediate solution (such as that obtained by ignoring the first motion at LPB). In general, the North American stations were better fitted by the strike-slip mechanism. The longer-period European stations were better fitted by the thrust mechanism; the shorter-period European stations could be fitted equally well by either solution. Closer inspection of the raw data revealed some evidence for source complexity that had also been suggested by Kroeger (1991). The first complex solution tested

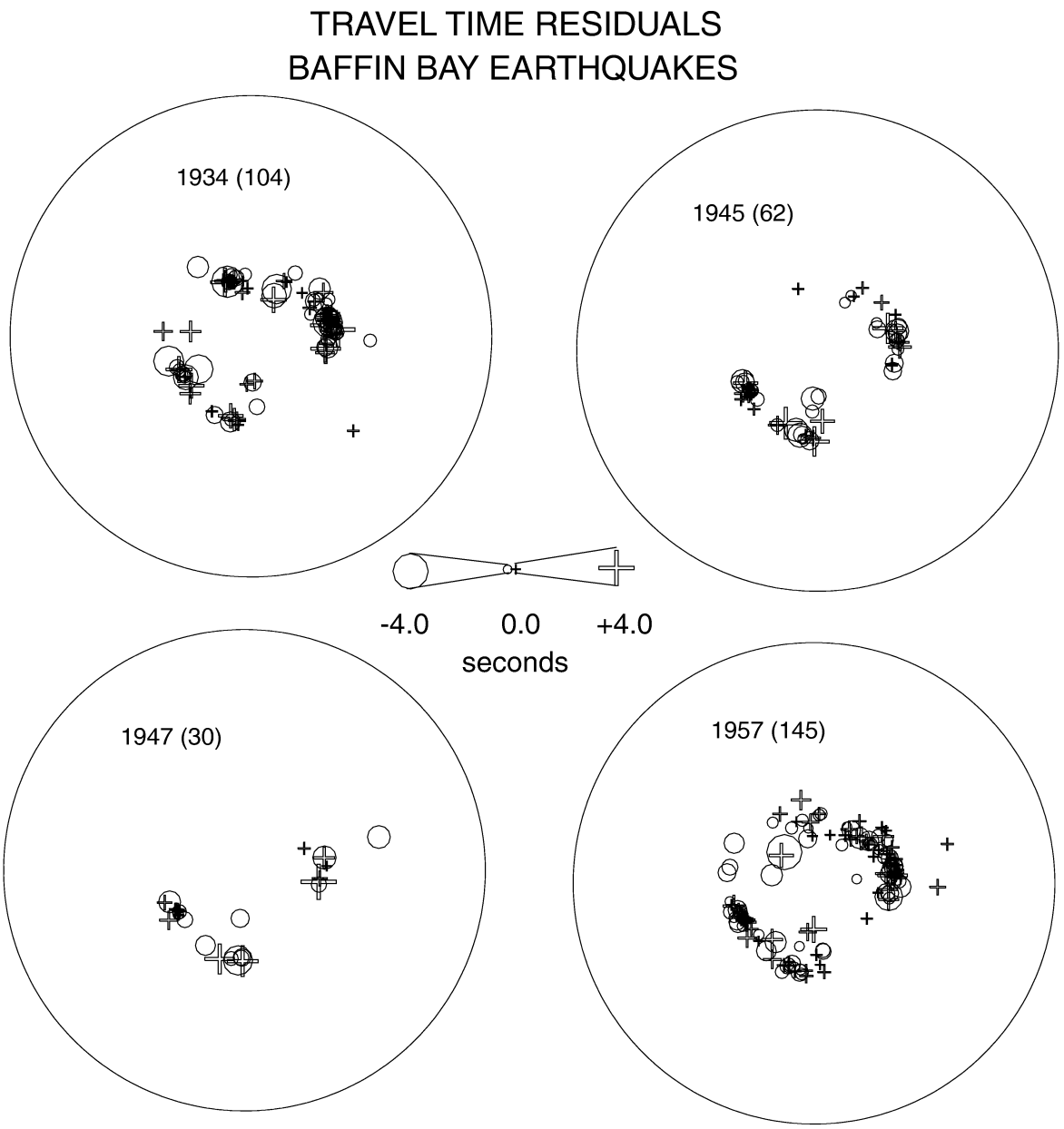

Figure 5. Traveltime residuals for other large earthquakes in Baffin Bay. The number of observations for each event is shown in parentheses. Symbol sizes are scaled to the size of the residual and are plotted on the focal sphere (lower hemisphere).

consisted of a small strike-slip event to satisfy the first motions followed by a larger thrust mechanism consistent with the previously suggested solution. The results were not very different from a simple thrust mechanism. The relative moment of the strike-slip subevent was gradually increased. A reasonable fit to the data was obtained when the moment of the strike-slip subevent was five times that of the thrust subevent. Complex sources with identical subevents were also modelled. Two strike-slip subevents will provide reasonable fits to the data but a source with different subevent mechanisms is marginally better. The data are not fitted by a solution consisting of two thrust subevents.

The second subevent occurs 10.5 s after the onset of the first. Adding a third subevent (also with a thrust mechanism) 21.5 s after the onset of subevent 1 improves the fit slightly. Table 4 summarizes the source parameters and Fig. 7 shows the data and synthetic seismograms. While the overall fit to the *P*-wave data is better than the fit to the *SH* waves, the *SH* synthetics do fit the major long-period characteristics of the seismograms. The higher-frequency component of the observed traces may result from structural complexities or may indicate that the attenuation is less than expected. The delay between subevents does not noticeably change from one station to another. Thus the rupture direction could not be determined. Most of the stations modelled lie close to the roughly E–W striking nodal plane. If the nearly N–S plane is the fault plane, large differences in subevent delays probably would not be observed by most stations, although the station at Toronto (TNT) would presumably have a

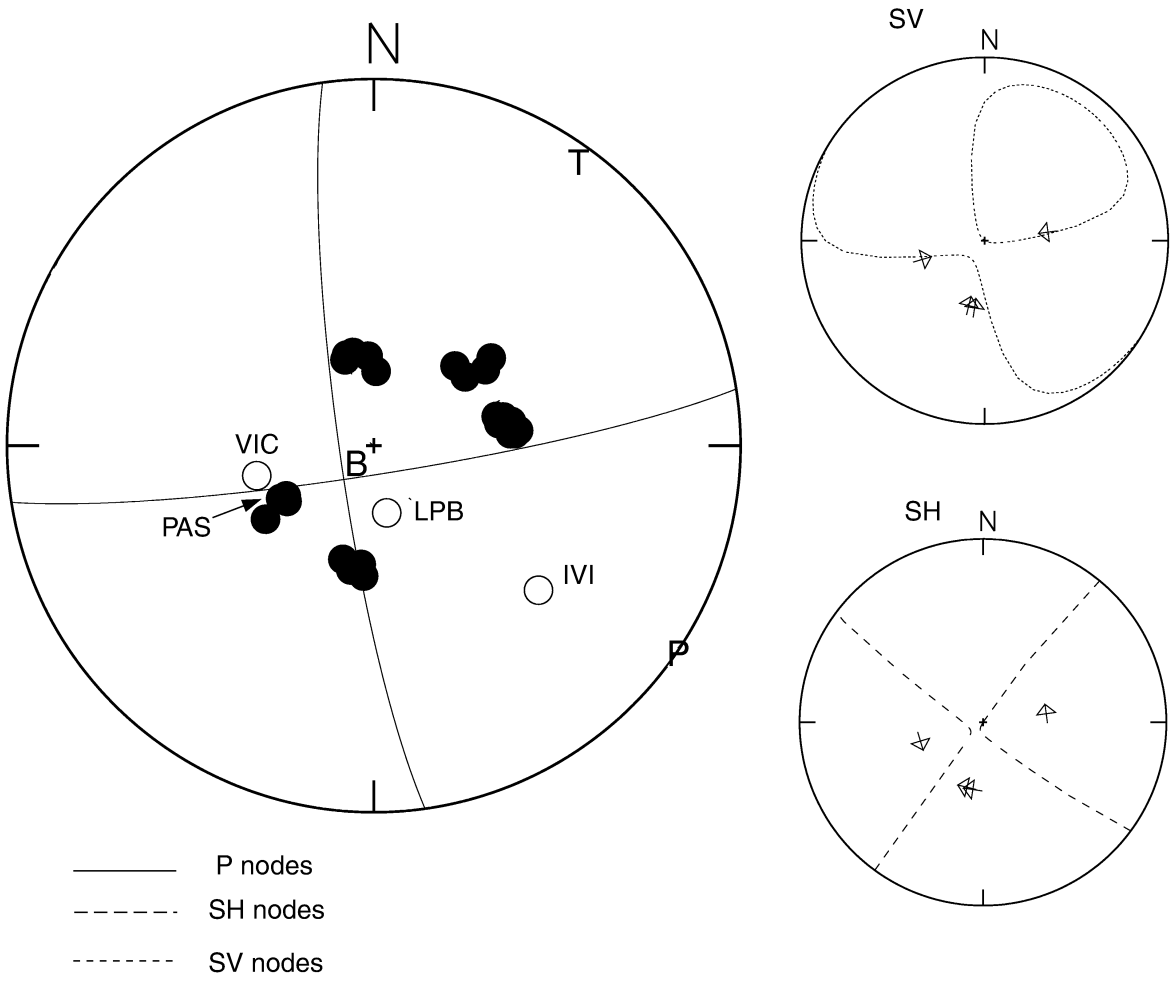

Figure 6. Focal mechanism derived from *P* first motions only. Lower-hemisphere projection. Solid circles represent compressional first motions and open circles dilatations. Stress axes (assuming the coefficient of friction is 0) and *S* nodal planes (dashed lines = SH; dotted lines = SV) are also shown. The *S* data are shown on the right with the arrows pointing in the direction of the first motion.

noticeably different delay than the others if the offset were significant.

Although the data are not adequate for the rupture direction or dimensions to be determined, the locations of subsequent large earthquakes in Baffin Bay allow for some speculation. Johnston (1993) gives an average rupture length of 70 km for stable continental earthquakes of moment magnitude 7.5. Even allowing for uncertainty, the 1934 (26 km), 1945 (22 km) and 1947 (4 km) earthquakes may lie within the rupture zone of the 1933 earthquake. All epicentres are to the south of the 1933 epicentre although the 1945 epicentre is to the southeast and the 1934 and 1947 epicentres are to the southwest. These observations suggest, but do not prove, that the NS nodal plane is the more likely fault plane. The azimuthal separation of the 1945 earthquake with respect to the 1934 and 1947 earthquakes is consistent with rupture on conjugate faults, but there is insufficient seismological and geological evidence to verify that this is the case. The 1957 earthquake, at a distance of 143 km, is assumed to lie outside of the 1933 rupture zone.

A graphical comparison at selected stations of the source models discussed above can be found in Fig. 8. The models tested can be compared quantitatively using the statistical F test. The *P* waves were used for the analysis. The fit of each synthetic to the corresponding seismogram is defined as the product of two ratios: the cross-correlation of the data and synthetic (with maximum amplitudes normalized) to the autocorrelation of the data, and the maximum amplitudes of the data and synthetic (with the larger value as the denominator). The mean fit for each model is listed in Table 5. The numbers themselves are less important than the differences between them. The preferred model has the highest mean fit; the simple thrust mechanism has the lowest. The F test (Table 4) shows that the difference between the preferred mechanism and the simple thrust mechanism is significant at the 90 per cent confidence level. The difference between the preferred mechanism and the complex all strike-slip solution is not statistically significant. The statistical significance of the difference between the preferred and other models lies between these two extremes and increases as the amount

Table 3. Summary of seismograms and instruments.

Station	Dist. (deg)	Az. (deg)	Instr.	Comps.	T_0 (s)	T_g (s)	h	V
Abisko (ABI)	27	54	G	Z,N,E	11.9	11.9	0.56	1100
Alma-Ata (AAA)	61	26	N	E	2.7	0.56	360	
Baku (BAK)	59	49	G	N	24.4	24.2	1.0	1307
				E	24.6	24.8	1.0	1450
De Bilt (DBN)	37	82	G	N,E	25	25	1.0	310
Irkutsk (IRK)	55	4	G	N	12.4	12.3	1.0	1639
Ivigtut (IVI)	14	134	W	Z,N,E	9.4	0.41	210	
Kew (KEW)	36	88	G	Z	12.9	12.9	1.0	308
				N	25.5	25.5	1.0	280
				E	24.7	24.7	1.0	280
Oak Ridge (ORT)	38	199	B	Z				
			MS	NW				
Ottawa (OTT)	28	189	MS	N,E	12		0.69	250
Pasadena (PAS)	46	237	WA	E,N	0.8		0.80	2800
			WA	E	6.0		0.80	800
			5–1.5	Z	0.5	1.5		
			S	N		0.2		
			S	N		34.9	1.0	200
			5–13	N	0.5	13.0		
Pulkovo (PUL)	37	55	G	Z	12.1	13.0	1.0	1428
				N	13.4	13.7	1.0	2249
				E	12.3	13.2	1.0	1928
Saskatoon (SAS)	26	235	M	N	9.0			61
				E	9.0			44
Toronto (TNT)	30	193	MS	N,E	12		0.69	150
Uccle (UCC)	38	84	W	Z	4.2		0.29	158
				N	7.3		0.28	160
				E	7.3		0.22	140
Victoria (VIC)	34	252	MS	N,E	12		0.69	250

Note.—B = Benioff, G = Galitzin, M = Mainka, MS = Milne–Shaw, N = Nikiforov, S = strain, T = torsion, W = Wiechert, WA = Wood–Anderson, numbers in this column indicate unnamed instruments identified by period. T_0 is the pendulum period; T_g is the galvanometer period; h is the damping constant; V is the instrument magnification (static magnification for mechanical instruments and maximum magnification for electromagnetic instruments) the damping ratio, may be calculated using the formula, $\epsilon = \exp[\pi h/(1-h^2)^{1/2}]$.

Table 4. Summary of source parameters of the 1933 Baffin Bay earthquake.

Origin time	1933 November 20 23:21:35.7 ± 0.2 s (UT)
Epicentre	73.07°N ± 4.5 km, 70.01° W ± 3.7 km
Moment (total)	$1.8 \pm 1.3 \times 10^{20}$ N m (10^{27} dyne cm)
M_w	7.3 ± 0.2 (maximum amplitude)
	7.4 ± 0.2 (sum of subevent moments)
M_s	7.3 (Gutenberg & Richter 1954)
m_b	7.2 ± 0.3
Subevent 1	
Strike	172° ± 2°
Dip	82° ± 2°
Rake	6° ± 3°
Depth	10 ± 2 km
Moment	$1.2 \pm 0.9 \times 10^{20}$ N m ($M_W = 7.3$)
Subevent 2	
Strike	190° ± 5°
Dip	30° ± 5°
Rake	62° ± 5°
Depth	10 ± 2 km
Moment	$2.4 \pm 1.7 \times 10^{19}$ N m ($M_W = 6.9$)
Delay	10.5 ± 0.5 s
Subevent 3	
Strike	190° ± 10°
Dip	30° ± 10°
Rake	62° ± 10°
Depth	10 ± 5 km
Moment	$3.6 \pm 2.6 \times 10^{19}$ N m ($M_W = 7.0$)
Delay	21.5 ± 1.0 s

of thrust motion in the other models increases, suggesting that the improved fit owing to a predominantly strike-slip mechanism is not a coincidence.

The scalar moment of the earthquake based on the sum of the subevent moments is $1.8 \pm 1.3 \times 10^{20}$ N m (10^{27} dyne cm), which corresponds to a moment magnitude, M_w, of 7.4 ± 0.2. If M_w is calculated directly from the peak amplitude at each station, it is 7.3 ± 0.2. The former is probably a more accurate measure of the energy released during the earthquake; the latter is more consistent with standard moment magnitude calculation practices. In any case, the moment magnitude is somewhat less than the previous estimate of 7.7 (Metzger & Johnston 1994) based on the M_s value, but is in close agreement with the value of 7.4 estimated by Johnston (1996a). Gutenberg & Richter (1954) calculated an M_s of 7.3. M_s was not recalculated in this study owing to a paucity of surface wave data. Using *P*-wave data from 11 stations, an m_b of 7.2 ± 0.3 was calculated. Note that this magnitude is not the high-frequency m_b commonly determined for recent earthquakes. The individual station data are tabulated in Bent (1998b).

The depth of all subevents, determined by modelling the depth phases, is 10 ± 2 km and agrees with the depth originally suggested by Lee (1937) based on *sP–P* times and with the more recent work of Kroeger (1991). A study by Stein *et al.* (1979) had suggested, based on the seismogram from Berkeley, that the hypocentral depth was 65 km. However, in an unpublished manuscript (Sleep *et al.* 1988), the authors revised the depth to 10 km.

DISCUSSION

While the predominantly strike-slip mechanism determined for the 1933 earthquake in this study contrasts with the conventional wisdom that Baffin Bay is a thrust faulting regime, there is additional evidence for strike-slip faulting in the region and some suggestion that the entire North American passive margin may be a strike-slip regime, differing from the onshore regions, which do appear to be dominated by thrust faulting, at least in Canada.

Using first-motion data from the ISS, fault plane solutions could be determined for the 1934 ($M_s = 6.5$) and 1957 ($M_s = 6.4$) Baffin Bay earthquakes (Fig. 9). The 1934 mechanism is very similar to that of the strike-slip subevent of the 1933 earthquake. Note that this solution is constrained by the reported dilatation from Nanking, which differs from the compressions reported by three other Chinese stations. The seismograms were not available to the present author. If that station is excluded, the focal mechanism cannot be constrained. However, *S* to *P* ratios at DBN are similar for the 1933 and 1934 earthquakes, providing some additional evidence for similar focal mechanisms. The mechanism for the 1957 event is somewhat different in orientation and has a higher component of thrust motion, although it is still a primarily strike-slip event (rake = 24°–27°). The ISS data set for this earthquake is large enough that the solution is well constrained and not dependent on a single station. Polarities from several stations (DBN, HBC, KLC, RES) were confirmed by the author. The 1957 earthquake is located further south than the

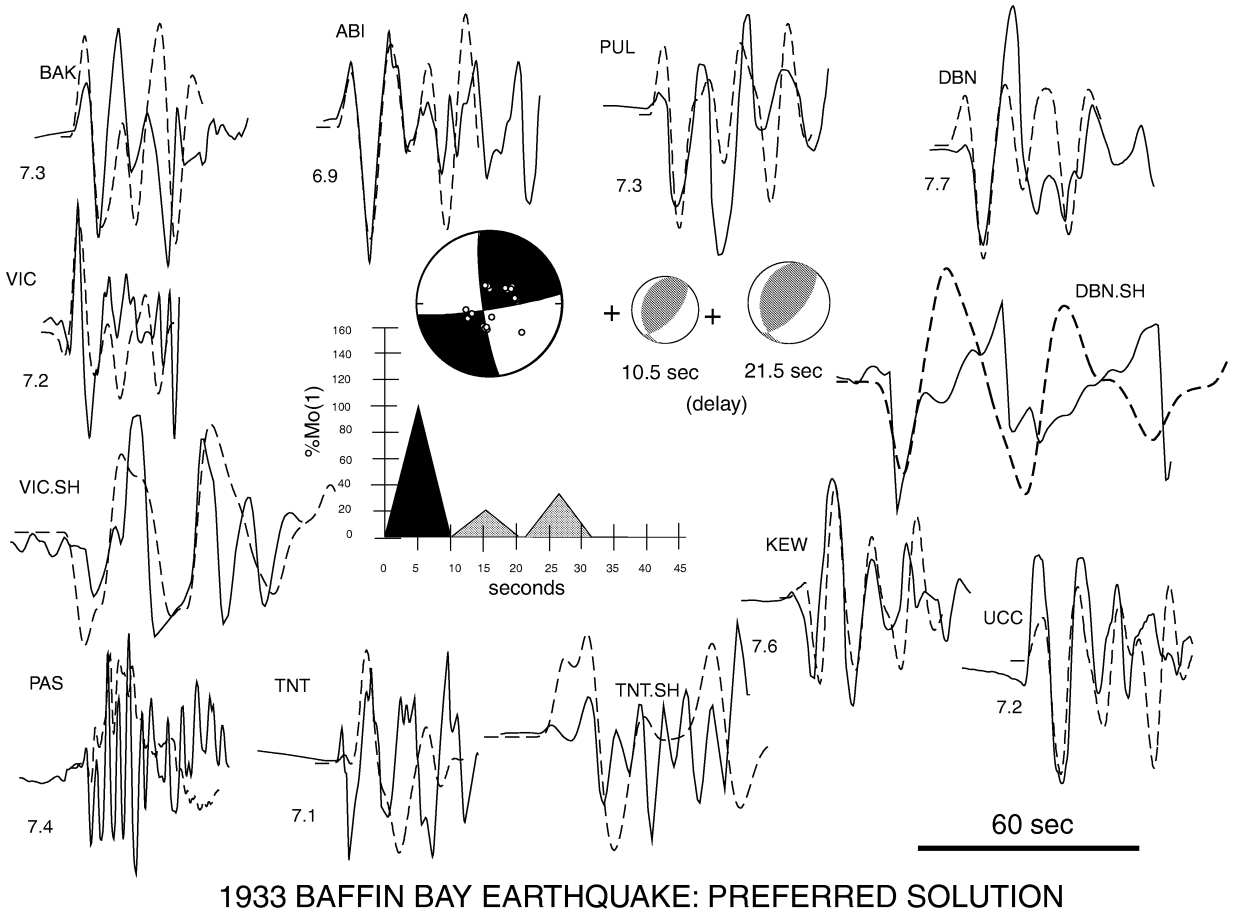

Figure 7. Waveform data (solid) and synthetic seismograms (dashed) for the preferred solution. Traces are for *P* waves unless indicated otherwise. All subevents have a focal depth of 10 km. The shading of the source time function corresponds to that of the fault plane solutions. The *y*-axis indicates the moment relative to the moment of subevent 1 (the largest). The number beside each data-synthetic pair indicates M_w calculated at that station. If two components are shown, M_w is the mean value.

other large Baffin Bay events but close to the epicentre of a moderate earthquake ($M_s = 5.1$) that occurred in 1976 and for which Stein *et al.* (1979) determined a primarily thrust mechanism. There were insufficient first-motion data to determine fault plane solutions for the 1945 ($M_s = 6.5$) and 1947 ($M_s = 6.0$) earthquakes. Possibly their mechanisms can be determined by future waveform analysis. Polarity data for the 1945 event are consistent with the 1933 (Fig. 9) mechanism. The 1947 event first motions are not, although they can be fit by many other strike-slip mechanisms. However, neither the 1945 nor the 1947 event is constrained to be a strike-slip event.

There is increasing evidence that the large eastern North American passive margin events further to the south are also strike-slip events (Fig. 10), as are many of the smaller earthquakes. Bent (1995a) used waveform modelling to obtain a primarily strike-slip mechanism for the 1929 ($M_s = 7.2$) Grand Banks earthquake. A smaller ($M_L = 4.4$) recent (1998 March 17) earthquake in the same area was also found to have a strike-slip mechanism (Bent & Perry 1999). A strike-slip mechanism is favoured based on geological data (Johnston 1996b) for the 1886 Charleston ($M_w \approx 7.3$) earthquake, although the mechanism cannot be considered well constrained. Some focal mechanisms for moderate earthquakes in the Labrador Sea (Bent & Hasegawa 1992) show evidence for strike-slip faulting, although there are also thrust- and normal-faulting events in that region.

On a global scale, passive margin earthquakes also appear to be predominantly, although certainly not exclusively, strike-slip events (Fig. 10). Of the 46 passive margin earthquakes included in the study of Johnston *et al.* (1994), 22 per cent are listed as strike-slip and 42 per cent have a larger strike-slip than dip-slip component with the dip-slip dominated events being nearly equally split between normal and thrust mechanisms. Strike-slip events are considered to be those for which the *B*-axis plunges at an angle of 65° or more. If the *B*-axis plunge is between 45° and 64°, the mechanism is considered predominantly strike-slip but with a significant dip-slip component. The percentage of strike-slip motion is calculated following the method of Frohlich (1992), which defines the proportion of strike-slip motion ($f_{\text{strike-slip}}$) as

$$f_{\text{strike-slip}} = \sin^2 \delta_B, \tag{1}$$

where δ_B is the plunge of the *B*-axis. Rakes $0° \pm 30°$ and $180° \pm 30°$ are generally considered to correspond to strike-slip earthquakes, $90° \pm 30°$ to thrust earthquakes, $-90° \pm 30°$ to normal, and everything in between to oblique. An advantage of using the *B*-axis instead of the rake angle is that the classification is independent of which nodal plane is the fault plane.

When only earthquakes of moment magnitude 6.0 or higher (nine events) are counted the percentages rise to 56 and 67 per cent, respectively, and the remaining events are all classified as normal with

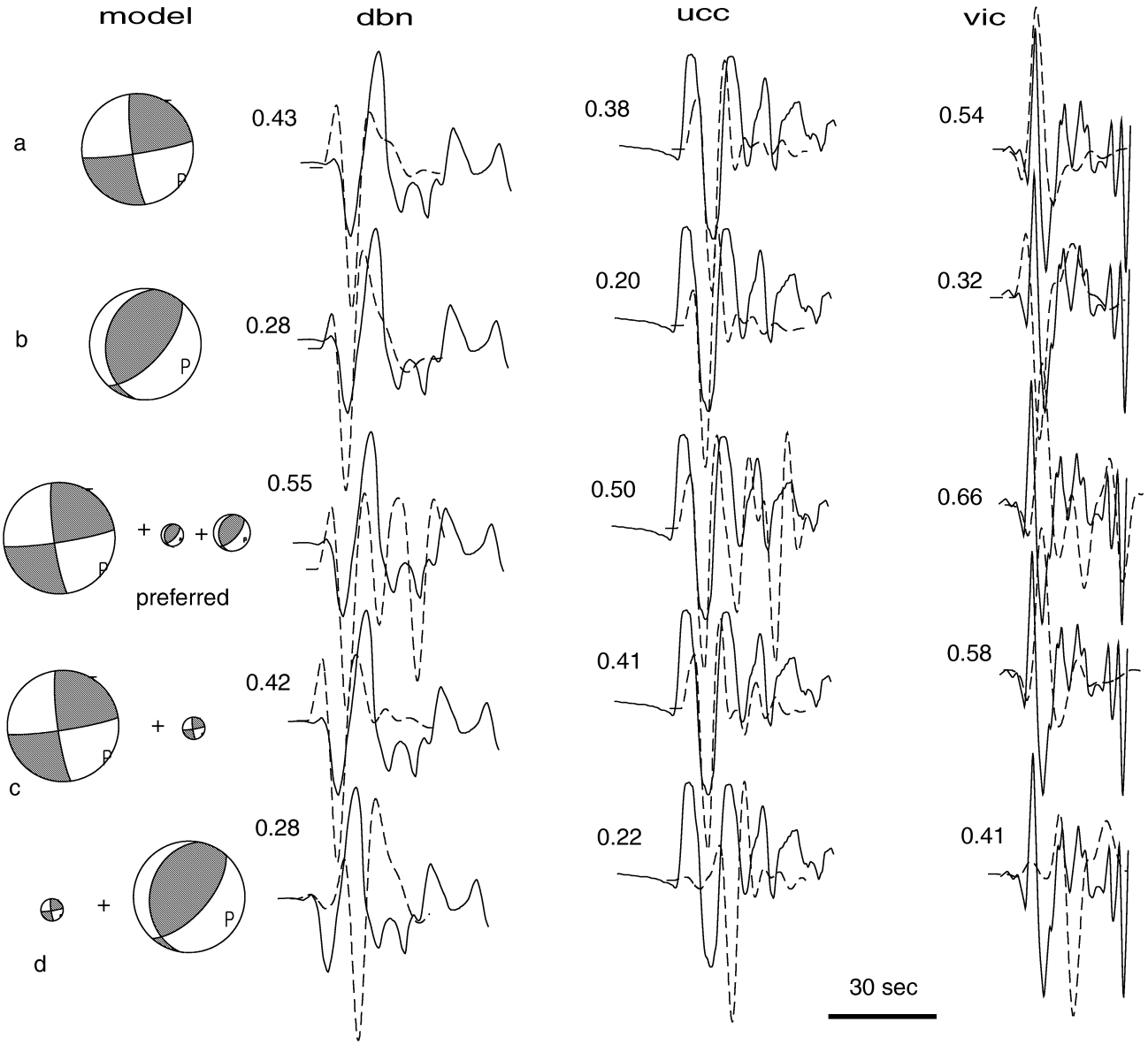

Figure 8. Waveforms (solid) and synthetic seismograms (dashed) at selected stations for five potential source models. All are teleseismic *P* waves. Maximum amplitudes have been normalized. The fit of each synthetic as defined in the text, which considers both waveform and amplitude, is noted. Model 'a' fits the beginning of the seismograms but misses the later phases. The same is true for model 'b' with respect to stations DBN and UCC. Models 'b' and 'd' clearly do not fit the VIC records. Nor does model 'd' provide a good fit to either DBN or UCC. Models 'c' and the preferred model fit the main characteristics at all stations. The differences between the two are small for UCC and VIC but the preferred model provides a noticeably better fit to DBN.

a strike-slip component. Note that the study of Johnston *et al.* (1994) considers the 1933 Baffin Bay earthquake to be a thrust event. I have taken the liberty of reclassifying it as a strike-slip event but otherwise have not touched the list either by changing the mechanisms of any events or by adding more events to the list. The 1934 and 1957 Baffin Bay earthquakes and the 1886 Charleston earthquakes were not included in the study, presumably because reliable focal mechanisms for these events were not available at the time. A discourse on global passive margin seismotectonics is beyond the intended scope of this paper, but it is worth noting that the data currently available suggest that margins originally formed by rifting appear to have been reactivated primarily by strike-slip faulting, an observation that contrasts with the accepted belief of a decade or so ago when these features were generally assumed to have been reactivated by thrust faulting.

Perhaps the best analogue to the 1933 Baffin Bay earthquake is a more recent, and therefore better recorded and intensely studied, event that occurred in 1998 within the Antarctic plate (1998 March 25, $M_w = 8.1$) and more than 200 km from a plate boundary. Like the Baffin Bay earthquake, the Antarctic earthquake was a large, shallow, intraplate, oceanic earthquake with a complex mechanism, in this case consisting of a strike-slip and an oblique-normal subevent (Antolik *et al.* 2000).

Considerable effort (for example, Hasegawa & Basham 1989; Stein *et al.* 1979, 1989) has gone into finding an explanation for the apparent juxtaposition of normal faulting on Baffin Island and

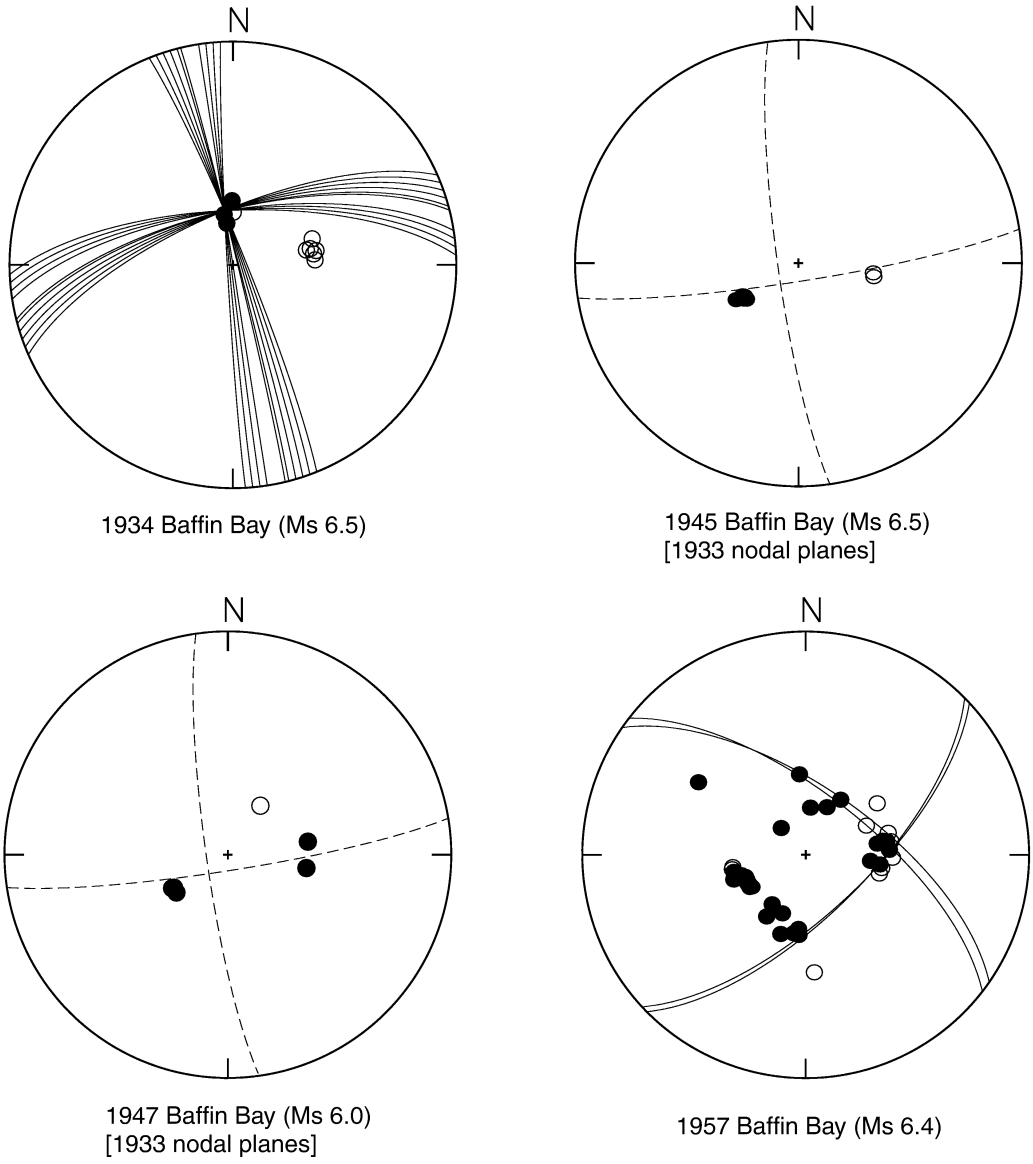

Figure 9. First-motion data (from the ISS) for large earthquakes in Baffin Bay subsequent to 1933. Fault plane solutions are shown for the 1934 and 1957 earthquakes. The mechanisms of the 1945 and 1947 events could not be constrained. For these two events the 1933 first-motion solution is indicated by dashed lines.

thrust faulting in Baffin Bay. While the results of the present study also show that faulting beneath Baffin Bay differs from that beneath Baffin Island, they suggest that the former is dominated by strike-slip faulting. Adjacent strike-slip and dip-slip regimes are easier to cope with as the assumed stress fields associated with them are generally more compatible. In this respect, Baffin Bay and Baffin Island earthquakes have a common feature in that the *P*-axes of most of them are oriented in an approximately northwest–southeast direction. The three Baffin Bay earthquakes (1933, 1934 and 1957) for which focal mechanisms were determined in this study all have NW–SE *P*-axes. The smaller 1976 earthquake, however, has its *P*-axis oriented NE–SW (Stein *et al.* 1979). Three out of four Baffin Island earthquakes (1963, 1970 and 1972) for which focal mechanisms are known also have NW–SE trending *P*-axes (Bent 1996a; Hashizume 1973), while the fourth (1993) has a NE–SW trending *P*-axis (Bent 1995b). Incidentally, the 1970 and 1993 events should actually be classified as strike-slip events with a normal component rather than as normal faulting events.

Although the 1933 earthquake has a complex mechanism, both the strike-slip and thrust subevents have similarly oriented *P*-axes—indicative of near horizontal compression in a northwest-southeast direction. While this stress direction differs from the assumed stress orientation (northeast–southwest compression) based on data primarily from southeastern Canada and the northeastern United States (Adams & Bell 1991; Zoback 1992), it is in good agreement with the stress field indicated by earthquake mechanisms in northeastern Canada and oil well breakout data from the Labrador shelf (Adams 1995; Bent 1996b). Richardson & Reding (1991) modelled various combinations of forces acting on the North American plate in an attempt to match the observed stress pattern. Most of the models they tested predict a change in the direction of maximum compression in the offshore regions north of approximately 50°, which corresponds

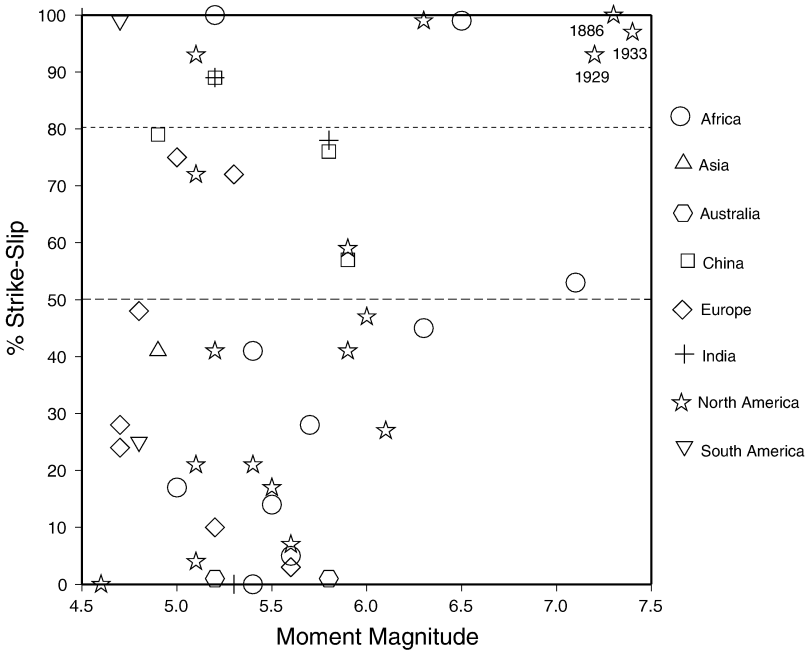

Figure 10. Strike-slip component of passive margin earthquakes worldwide. The focal mechanism and event selection are from Johnston *et al.* (1994) with two exceptions: the focal mechanism for the 1933 Baffin Bay earthquake is the one obtained in this paper, and the 1886 Charleston earthquake has been added using the focal mechanism of Johnston (1996b). The three largest North American passive margin earthquakes are identified by year of occurrence. Earthquakes plotting above the dotted line are considered pure strike-slip (*B*-axis plunge 65°–90°. Those potting between the dotted and dashed lines are predominantly strike-slip but have a significant dip-slip component (*B*-axis plunge 45°–64°.

Table 5. Statistical comparison of source models.

Model	χ_i	V	V_B	V_W	F	P_F
a (1 ss)	0.49	0.73	0.02	0.57	0.51	0.50
b (1 thr)	0.40	0.69	0.12	0.57	3.21	0.10
c (2 ss)	0.51	0.78	0.01	0.77	0.23	0.75
d (sm ss + lg thr)	0.42	0.70	0.09	0.61	2.31	0.25
Preferred	0.56					

Note.—Models as defined in text and Fig. 9. χ_i is the mean fit for model i. V is the total variation. V_B is the variation between model i and the preferred model. V_W is the variation within model i. F is the F-ratio defined as.

$$\frac{V_B/(a-1)}{V_W/a(b-1)},$$

where $a = 2$ (number of models compared) and $b = 9$ (number of data points (i.e. stations) in each model). P_F is the probability that the difference between model i and the preferred model is based on chance (obtained from Table 26.9 of Abramowitz & Stegun (1965) as abridged below) for $\nu_1 = 1$ and $\nu_2 = 16$ degrees of freedom where ν_1 is $a - 1$ and ν_2 is $a(b-1)$: $F_{0.01} = 8.53$ $F_{0.1} = 3.05$ $F_{0.25} = 1.42$ $F_{0.5} = 0.476$ $F_{0.75} = 0.105$.

to the conclusions of Bent & Hasegawa (1992) based on earthquakes in the Labrador Sea. Those models that did not predict a change in stress orientation generally did not provide a good fit to the observed stresses elsewhere in the plate. At least to a first degree, the stresses predicted by modelling are in agreement with those predicted by earthquake focal mechanisms.

CONCLUSIONS

An analysis of waveforms recorded for the 1933 Baffin Bay earthquake has determined that it was a shallow (10 km) complex event consisting of a large strike-slip subevent followed by two predominantly thrust subevents. An instrumental moment magnitude of 7.4 was calculated. The focal mechanism contrasts with the established belief that Baffin Bay is dominated by thrust faulting but is consistent with the concept that the predominant mechanism in Baffin Bay differs from that of Baffin Island. First-motion focal mechanisms for two other large Baffin Bay earthquakes (1934 and 1957) provide additional evidence for strike-slip faulting, although one of the solutions (1934) is constrained primarily by a reported polarity from one station and should be interpreted with caution.

The results of this study combined with recent analyses of the two other largest eastern North American passive margin earthquakes—1929 Grand Banks (Bent 1995a) and 1886 Charleston (Johnston 1996b)—suggest that the entire passive margin may be dominated by strike-slip faulting (Fig. 10). However, this conclusion is based on three earthquakes separated by thousands of kilometres, and some care must be taken not to overinterpret the data. More variation is observed among the focal mechanisms of smaller passive margin earthquakes. At the same time, there is increasing evidence (Johnston *et al.* 1994) that large, passive margin earthquakes in general may be predominantly strike-slip events.

ACKNOWLEDGMENTS

I thank the numerous people who sent me seismograms, and John Adams, John Cassidy and Diane Doser for their constructive reviews. Geological Survey of Canada contribution no 2001020.

REFERENCES

Abramowitz, M. & Stegun, I.A., 1965. *Handbook of Mathematical Functions with Formulas, Graphs and Mathematical Tables*, Dover, New York, p. 1046.

Adams, J., 1995. The Canadian crustal stress database: a compilation to 1994 Part 1, *Geol. Surv. Canada Open File 3122,* p. 38.

Adams, J. & Bell, S., 1991. Crustal stresses in Canada, in *Neotectonics of North America Decade Map,* Vol. 1, pp. 376–386, eds Slemmons, D.B., Engdahl, E.R., Zoback, M.D. & Blackwell, D.D., Geology Society of America, Boulder, CO.

Antolik, M., Kaverina, A. & Dreger, D.S., 2000. Compound rupture of the great 1998 Antarctic earthquake, *J. geophys. Res.,* **105,** 23 825–23 838.

Basham, P.W., Forsyth, D.A. & Wetmiller, R.J., 1977. The seismicity of northern Canada, *Can. J. Earth Sci.,* **14,** 1646–1667.

Basham, P.W., Weichert, D.H., Anglin, F.M. & Berry, M.J., 1982. New probabilistic strong seismic ground motions maps of Canada: A compilation of earthquake source zones, methods and results, *Earth Physics Branch Open File 82–33*, p. 205.

Basham, P., Halchuk, S., Weichert, D. & Adams, J., 1997. New seismic hazard assessment for Canada, *Seism. Res. Lett.,* **68,** 722–726.

Bent, A.L., 1995a. A complex double-couple source mechanism for the Ms 7.2 1929 Grand Banks earthquake, *Bull. seism. Soc. Am.,* **85,** 1003–1020.

Bent, A.L., 1995b. Source parameters of the 1963 Mw 6.1 Baffin Island earthquake, *Geol. Surv. Canada Open File 3146,* p. 53.

Bent, A.L., 1996a. Another look at the 1963 Mw 6.1 Baffin Island earthquake, *Seism. Res. Lett.,* **67,** 64–71.

Bent, A.L., 1996b. The stress field along the northeastern Canadian margin: New insight from earthquake focal mechanisms (abstract), *Seism. Res. Lett.,* **67,** 32.

Bent, A.L., 1998a. Revised epicenters for large historical earthquakes in Baffin Bay, *Geol. Surv. Canada Open File 3644,* p. 44.

Bent, A.L., 1998b. Seismograms for historic Canadian earthquakes: The 20 November 1933 Baffin Bay earthquake, *Geol. Surv. Canada Open File 3645,* p. 29.

Bent, A.L. & Hasegawa, H.S., 1992. Earthquakes along the northwestern boundary of the Labrador Sea, *Seism. Res. Lett.,* **63,** 587–602.

Bent, A.L. & Perry, C., 1999. Focal mechanisms for eastern Canadian earthquakes: 1 January 1996–30 June 1998, *Geol. Surv. Canada Open File 3698,* p. 148.

Dziewonski, A.M. & Anderson, D.L., 1981. Preliminary reference Earth model, *Phys. Earth planet. Inter.,* **25,** 297–356.

Frohlich, C., 1992. Triangle diagrams: ternary graphs to display similarity and diversity of earthquake focal mechanisms, *Phys. Earth planet. Inter.,* **75,** 193–198.

Futterman, W.I., 1962. Dispersive body waves, *J. geophys. Res.,* **67,** 5279–5291.

Gutenberg, B. & Richter, C.F., 1954. *Seismicity of the Earth and Related Phenomena,* Princeton University Press, Princeton, NJ, p. 310.

Hasegawa, H.S. & Basham, P.W., 1989. Spatial correlation between seismicity and postglacial rebound in eastern Canada, in *Earthquakes at North-Atlantic Passive Margins: Neotectonics and Postglacial Rebound,* pp. 483–500, eds Gregersen, S. & Basham, P.W., Kluwer, Dordrecht.

Hashizume, M., 1973. Two earthquakes on Baffin Island and their tectonic implications, *J. geophys. Res.,* **78,** 6069–6081.

Jackson, H.R., Keen, C.E., Falconer, R.K.H. & Appleton, K.P., 1979. New geophysical evidence for sea-floor spreading in Baffin Bay, *Can. J. Earth. Sci.,* **16,** 2122–2135.

Johnston, A.C., 1993. Average stable continental earthquake source parameters based on constant stress drop scaling, *Seism. Res. Lett.,* **64,** 261.

Johnston, A.C., 1996a. Seismic moment assessment of earthquakes in stable continental regions-I. Instrumental seismicity, *Geophys. J. Int.,* **124,** 381–414.

Johnston, A.C., 1996b. Seismic moment assessment of earthquakes in stable continental regions-III. New madrid 1811–1812, Charleston 1886 and Lisbon 1755, *Geophys. J. Int.,* **126,** 314–344.

Johnston, A.C., Coppersmith, K.J., Kanter, L.R. & Cornell, C.A., 1994. *The Earthquakes of Stable Continental Regions Volume 1: Assessment of Large Earthquake Potential,* EPRI Rep. TR-102261-V1, Electric Power Research Inst., Palo Alto, California, 4-15–4-18.

Keen, M.J., Johnson, J. & Park, I., 1972a. Geophysical and geological studies in eastern and northern Baffin Bay and Lancaster Sound, *Can. J. Earth. Sci.,* **9,** 689–708.

Keen, C.E., Barrett, D.L. & Manchester, K.S., 1972b. Geophysical studies in Baffin Bay and some tectonic implications, *Can. J. Earth. Sci*., **9,** 239–256.

Kroeger, G.C., 1991. The 20 November 1933 Baffin Bay earthquake: A new focal mechanism solution, *EOS, Trans. Am. geophys. Un.,* **72,** *Spr. Mtng Suppl.,* abstract 189.

Langston, C.A. & Helmberger, D.V., 1975. A procedure for modeling shallow dislocation sources, *Geophys. J. R. astr. Soc.,* **42,** 117–130.

Lee, A.W., 1937. On the travel time of seismic waves from the Baffin Bay earthquake of November 20, 1933, *Meteorol. Office Geophys. Mem. No. 74,* London, p. 21.

Metzger, A.G. & Johnston, A.C., 1994. The stable continental region earthquake database, in *The Earthquakes of Stable Continental Regions: Assessment of Large Earthquake Potential,* Vol. 4, p. NA-148, ed. Schneider, J.F., EPRI Rep. TR-102261, *Electric Power Res. Inst.,* Palo Alto, California.

Qamar, A., 1974. Seismicity of the Baffin Bay region, *Bull. seism. Soc. Am.,* **64,** 87–98.

Rajko, N. & Linden, N., 1935. On the earthquake of 20 XI 1933 in the Baffin Bay and on the distribution of epicentres in the Arctic, *Acad. Sci. USSR Institute of Seism. Pub. No. 61,* 1–8 (in Russian).

Richardson, R.M. & Reding, L.M., 1991. North American plate dynamics, *J. geophys. Res.,* **96,** 12 201–12 223.

Roest, W.R. & Srivastava, S.P., 1989. Sea-floor spreading in the Labrador Sea: a new reconstruction, *Geology,* **17,** 1000–1003.

Sleep, N.H., Kroeger, G. & Stein, S., 1988. Canadian passive margin stress field inferred from seismicity, Unpublished Manuscript.

Snoke, J.A., Munsey, J.W., Teague, A.G. & Bollinger, G.A., 1984. A program for focal mechanism determination by combined use of polarity and $SV-P$ amplitude data (abstract), *Earthquake Notes,* **55,** 15.

Srivastava, S.P., Falconer, R.K.H. & MacLean, B., 1981. Labrador Sea, Davis Strait, Baffin Bay; geology and geophysics—a review, in *Geology of the North Atlantic Borderlands,* Vol. 7, pp. 333–398, eds Kerr, J.W. & Fergusson, A.J., Canadian Soc. of Petroleum Geologists Memoir.

Stein, S., Sleep, N.H., Geller, R.J., Wang, S.-C. & Kroeger, G.C., 1979. Earthquakes along the passive margin of eastern Canada, *Geophys. Res. Lett.,* **6,** 538–540.

Stein, S., Cloetingh, S., Sleep, N.H. & Wortel, R., 1989. Passive margin earthquakes, stresses and rheology, in, *Earthquakes at North-Atlantic Passive Margins: Neotectonics and Postglacial Rebound,* pp. 231–259, eds Gregersen, S. & Basham, P.W., Kluwer, Dordrecht.

Weichert, D.H. & Newton, J.C., 1970. Epicentre determination from first arrival times at Canadian stations, *Seismology Series of the Earth Physics Branch no. 59,* Ottawa, p. 16.

Wetmiller, R.J., 1974. Crustal structure of Baffin Bay from the earthquake-generated Lg phase, *Can. J. Earth. Sci.,* **11,** 123–130.

Zoback, M.L., 1992. Stress field constraints on intraplate seismicity in eastern North America, *J. geophys. Res.,* **97,** 11 761–11 782.